A microfluidic-SERSplatform for isolation and immuno-phenotyping of antigen specific T-cells

Shuvashis Dey[a] Ramanathan Vaidyanathan[a] K. Kamil Reza[a] Jing Wang[a] Yuling Wang[a] Hendrik J. Nel[b] Soi-Cheng Law[b] Jennifer Tyler[b] Jamie Rossjohn[cde] Hugh H. Reid[fg] Abu AliIbn Sina[a] Ranjeny Thomas[b] Matt Trau[ah]

a. Centre for Personalised Nanomedicine, Australian Institute for Bioengineering and Nanotechnology, The University of Queensland, QLD 4072, Australia
b. University of Queensland Diamantina Institute, Translational Research Institute, QLD 4072, Australia
c. Infection and Immunity Program, The Department of Biochemistry and Molecular Biology, Biomedicine Discovery Institute, Monash University, Clayton, Victoria 3800, Australia
d. Australian Research Council Centre of Excellence for Advanced Molecular Imaging, Monash University, Clayton, Victoria 3800, Australia
e. Institute of Infection and Immunity, Cardiff University, School of Medicine, Heath Park, Cardiff CF 14 4XN, United Kingdom
f. Infection and Immunity Program, The Department of Biochemistry and Molecular Biology, Biomedicine Discovery Institute, Monash University, Clayton, Australia
g. Australian Research Council Centre of Excellence in Advanced Molecular Imaging, Monash University, Clayton, Australia
h. School of Chemistry and Molecular Biosciences, The University of Queensland, QLD 4072, Australia

HIGHLIGHTS

A microfluidic platform for the specific isolation of antigen specific T-cells with high sensitivity (0.005%).

Release of T-cell from the device using a single point direct current (DC) pulse.

Monitoring TCR expression heterogenity on antigen specific T-cells using SERS.
T-cell receptor expression analysis on individual T-cells using SERS-nanotags.

ABSTRACT

T-cells play a major role in host defense mechanisms against many diseases. With the current growth of immunotherapy approaches, there is a strong need for advanced technologies to detect and characterize these immune cells. Herein, we present a simple approach for the isolation of antigen specific T-cells from the complex biological sample based on T-cell receptor (TCR) and peptide major histocompatibility complex (pMHC) interaction. Subsequently, we characterize those antigen specific T-cells by profiling TCR expression heterogeneity. Our approach utilizes an alternating current electrohydrodynamic (ac-EHD) based microfluidic platform for isolation and surface enhanced Raman scattering (SERS) for TCR expression profiling. The use of ac-EHD enables specific isolation of T-cells by generating a nanoscopic shear force at the double layer of the sensing surface which enhances the frequency of pMHC and TCR interactions and consequently shears off the nonspecific targets. TCR expression profiling of the isolated T-cells was performed by encoding them with SERS-labelled pMHCs followed by SERS detection in bulk as well as in single T-Cell. In proof-of-concept experiments, 56.93 ± 7.31% of the total CD4+T-cells were captured from an excess amount of nonspecific cells (e.g., PBMCs) with high specificity and sensitivity (0.005%). Moreover, TCR analysis data using SERS shows the heterogeneity in the T-cell receptor expression which can inform on the activation status of T-cells and the patient's response to immunotherapy. We believe that this approach may hold potential for numerous applications towards monitoring immune status, understanding therapeutic responses, and effective vaccine development.

1. INTRODUCTION

T-cell mediated immunotherapy has gained wide attention over the years for its success in disease management. Monitoring the therapeutic response in patients requires characterization of antigen specific T-cells to understand their potential role in immune response [1]. The mechanism that plays a major role in the regulation of downstream immune responses is usually characterized by the interaction of T-cell receptor (TCR) with antigenic peptides presented by the major histocompatibility complex (pMHC) on the surface of antigen presenting cells (APCs) [[2], [3], [4]]. This interaction initiates the activation and maturation of T-cells and triggers the adaptive host immune response towards specific antigens [5]. Thus the characterization of pMHC-TCR interactions is of fundamental importance to better understand the immune system and to facilitate the development of antigen-specific therapeutic formulations and vaccines for disease control [6,7]. However, TCR specificities towards various antigenic peptides presented by MHC molecules (class I and class II) are diverse, antigen-specific cells are rare in circulation and most interactions are of low affinity (K_d~ 0.1–500 μM) which makes their detection extremely challenging [8]. Thus, a suitable biosensor platform that can enable the identification of T-cells using pMHC-TCR interactions with high sensitivity and specificity is highly desirable.

Development of soluble pMHC multimers has aided the analysis of specific T-cells using conventional flow cytometry [[9], [10], [11], [12], [13]]. For example, Greten and co-workers utilized pMHC multimers in flow cytometry assay to detect HTLV-1 Tax11–19-specific CD8 + T cells in peripheral blood of HAM/TSP patients [10]. Furthermore, the use of different combinatorial approaches has enabled to detect multiple antigen specific T-cells simultaneously by different cytometry based approaches. Utilizing 10 metal labels in combinations for pMHC tetramer based staining, Newell et al. demonstrated the applicability of mass cytometry for the screening of 109 different antigen specific T-cells in one sample [11]. More recently, Bentzen et al. developed a DNA barcoding assay technique by tagging different pMHC molecules with signature DNA tags. This allows the screening of T-cells with more than one thousand different peptide loaded MHCs [12]. Although cytometry-based methods provide multiplexed analysis of T-cell populations, they are limited by sample volume, optical encoding, expensive instruments and analysis time[14]. Alternative methods including Enzyme-Linked ImmunoSpot (ELISpot) and Enzyme-Linked immunosorbent assay (ELISA) require prior assumption of the secretory profile of the activated T-cells, and therefore isolation of antigen specific T-cells using these methods are challenging [15]. To address these shortcomings, a limited number of array-based approaches have been developed (Table 1) for T-cell analysis by functionalizing the array surface with pMHC multimers [14,[16], [17], [18], [19], [20]]. In a modified microarray approach, Shen et al. combined magnetic assisted cell sorting with the functional assay for simultaneous sorting and characterization of antigen specific T-cells. They developed an artificial antigen-presenting cell microplate (termed AAPC-microplate) containing pMHCs and anti-CD28 co-labeled magnetic beads and anti-cytokine antibodies in each well which facilitated parallel isolation and functional characterization of T-cells [21]. In a most recent report, Zhu et al. developed graphene-based MHC–peptide multimers (HRGO/ pMHC multimers) by loading pMHC molecules on hemin functionalized reduced graphene oxide (HRGO) for T-cell analysis. This approach allows more pMHCs per multimeric complex which could be potentially advantageous for T-cell analysis with the weak affinity between pMHC and T-cell receptors [22]. Further, this method utilizes a catalytic reaction between HRGO and tetramethylbenzidine (TMB)/H_2O_2 for detection which avoids the common problem of photo-bleaching associated with fluorescence based detection approaches. Although microarray platforms demonstrated numerous advantages over flow cytometry, the array techniques require a large number of target cells and it is difficult to control the flow conditions and appropriate pMHC orientation on array surface which limits their sensitivity and specificity [18,[17], [18], [19], [20],23].

In recent years, microfluidic techniques have become attractive assay platforms for cellular analysis due to their ability to facilitate faster target diffusion and control over the fluidic process to cater low-affinity interactions upon alteration of fluid flow [[24], [25], [26], [27]]. We have recently developed a microfluidic platform based on alternating current (ac) electrohydrodynamic (ac-EHD)-induced fluid flow phenomenon to improve the sensitivity and specificity of biomolecule detection [26,27]. However, microfluidic techniques mostly use fluorescence labeling for detecting the captured targets in the device under a fluorescence microscope. Recently, Surface enhanced Raman scattering (SERS) have become more attractive detection reagents over fluorescence-based detection, because of their high photostability, sensitivity (down to single-cell detection) and extensive multiplexing capability [28,29]. We have recently reported a SERS based report that can monitor the change in cellular phenotypic expression of circulating tumor cells during drug treatment [30]. Thus, a SERS technique integrated with the microfluidic platform may potentially facilitate the characterization of T-cells using pMHC-TCR interactions and overcome the above-stated limitations associated with current techniques.

In this study, we develop a simple microfluidic-SERS platform for isolation and characterization of antigen specific T-cell. The platform utilizes specific pMHC-TCR interaction using an ac-EHD enabled microfluidic device for specific T-cell isolation and SERS technique to characterize TCR distribution in both bulk population and single T-cells. The integration of ac-EHD induced fluid micromixing inside the microfluidic channels enhances the collision between target T-cells and the pMHC functionalized surface; hence significantly improve the capture efficiency in comparison to the pressure driven flow system. Our approach also shows high specificity and sensitivity (0.005%) for capturing T-cells from complex biological samples (PBMCs). Moreover, on-chip labelling of the isolated T-cell with SERS-pMHCnanotags obviates the need of multiple wash steps associated with cell labelling which is often unsuitable for rare cell analysis due to the loss of target cells during washing. Subsequent cell release using single point direct current (DC) pulse permits the SERS screening of average TCR expression level from the released T-cells in bulk as well as empowered the system to screen single T-cell TCR expression which is currently difficult to achieve with existing techniques. Finally, our method is simple, multiplexable and requires small sample volume to operate which we believe can potentially be suitable for clinical applications.

2. EXPERIMENTAL SECTION

2.1. Reagents

Immunoassay reagents were obtained from Abcam (Australia), R&D/Life Technologies (Burlington, ON), Thermo-Fisher Scientific (Australia), Invitrogen (Australia) and Altor BioScience Corporation (USA). All other reagents unless stated otherwise were purchased from Sigma-Aldrich (Australia). Commercial reagents from Altor BioScience Corporation include p53 (aa264-272) Star™Multimer (human leukocyte antigen (HLA)-A2.1 restricted), and biotinylated p53-HLA-A2 monomers. Biotinylated $HA_{306-318}$-HLA-DRB1*04:01 monomers and Streptavidin-PE (phycoerythrin)tetramers (pMHC II) were synthesised as previously described [26].

2.2. Device design and fabrication

This chip contains 264 pairs of asymmetric planar electrodes (electrode sizes: 100 μm and 400 μm) connected by two gold connecting pads act as cathode and anode(Figure S1). Small and large electrodes in a pair are separated by 50 μm and the distance between two pairs is 150 μm. The electrode geometry in our device was optimized to engender effective ac-EHD fluid flow and maintained uniformly throughout each channel as: $r_0/d_2 = 0.125$, $r_1/d_2 = 0.375$, $d_1/d_2 = 0.25$,

respectively [27]. The device works on the principle of electric field induced fluid flow phenomena as described in the previous literature [27,31,32].

Device fabrication was performed using standard photolithography. Detailed procedures of device fabrication are available in the supplementary information(Figure S2).

2.3. Device functionalization

Initially, clean device was incubated with biotinylated BSA solution (250 µl of 200 µg/mL) at 37 °C for 2 h, then with streptavidin solution (100 µg/mL in PBS) for 1 h at 37 °C. Finally, biotinylatedp MHC monomer was added and incubated at 4 °C for 1 h (Figure S3). For tetramer functionalization, after streptavidin attachment, biotinylated anti-PE was incubated for 1 h and then PE-labeled pMHC tetramer solution (1 µg/mL) was added to the anti-PE functionalized device and incubated (4 °C) for 1 h (Figure S4). The functionalized device was washed with PBS (1 mM, pH 7.0) and incubated with BSA solution. PDMS defined channel was attached to the device and the device was connected to a signal generator to perform experiments. The storage performance of the device was tested by keeping the device in a vacuum sealed box from 0 to 4 weeks which showed high reproducibility in capturing targets even after 4 weeks of storage time (Figure S5).

2.4. Cell culture and flow cytometry analysis

Hemagglutinin$_{306\text{-}318}$ (HA) specific- $CD4^+$T-cell clones were generated as described previously [33]. A detailed description of $CD4^+$ T-cell is described in the supplementary section. Control SKBR-3 cells were maintained in RPMI 1640 growth medium supplemented with 10% FBS, 1% penicillin and 1% glutamax and grown in 5% CO_2 at 37 °C.

2.5. Cell capture, labelingand detection

CD4+T-cells were labeled with DiO (3,3′-Dioctadecyloxacarbocyanine Perchlorate) fluorescence dye by incubating at 37 °C for 10 min (5 µL of DiO dye for 100,000 cells/sample). After labeling, cells were washed with PBS buffer to remove any staining debris.

Sample containing a designated number of cells in PBS (200 µL) ran through the device under optimal ac-EHD field (f = 600 Hz, V_{pp} = 100 mV). Captured cells were then optically detected under a fluorescence microscope (Figure S3). For TCR distribution analysis, captured cells were incubated (45 min, on chip) with SERS labelledpMHC tetramer (see supplementary information for SERS-pMHC tag preparation), then released by applying a reductive DC pulse (1.4 V for 200 s) across the capture domain, washed with PBS and collected from the outlet (1 mM, pH 7.0) [26]. Recovered cells were energized with a single laser (SnIR IM-52 portable Raman microscope) to record the SERS spectra from T-cells (Figure S4). To this end, individual T-cell was scanned under Raman microscope and SERS intensity of each cell was divided by the total cell area to get average SERS intensity for a given cell.

3. RESULTS AND DISCUSSION

3.1. Immunochip for T-cell capture and phenotypic analysis

For isolation and immune-phenotyping of T-cells, we fabricated an ac-EHD microfluidic chip containing an array of asymmetric electrode pairs across the whole channel (Figure 1, S1). This new device comprises a serpentine channel with U shaped turns in each corner that facilitates smooth fluid flow across the channel and minimized nonspecific adsorption of molecules in the corners. The long serpentine PDMS-based microchannel provided additional fluid micromixing for

the improved interaction of target cells with the functionalized surface under ac-EHD. Figure 1 depicts the detailed working principle of immunochip for T-cell analysis. In brief, the application of ac potential across asymmetric electrode pairs induces a non-uniform electric field (E). It leads to asymmetric distribution of charges between the electrodes. Due to the asymmetric charge layer formation on electrode surfaces, the resultant force F ($F = \rho E_t$, where ρ = charge density, E_t = tangential component of E) on larger electrode become stronger than that of the smaller electrode (F_s ;$F_l > F_s$). This variation in localized body forces pushes sample fluid inside the microchannel from smaller to the larger electrode. Simultaneously, it generates micromixing that enhances interactions of T-cells with pMHC functionalized surface - thereby increases capture efficiency. At the same time the force also assists to drag off and remove loosely bounded nonspecifically adsorbed molecules from the device surface [26]. Post capture, T-cells were labelled onchip by flowing SERS nanotags (SERS nanoparticle tagged with pMHC molecules) under the same ac-EHD condition to allow better interaction of captured T-cells with SERS-pMHCnanotags. Subsequently, SERS tagged T-cells were released from the capture domain by the application of a single point DC pulse that broke the thiol bond between capture molecules with gold electrodes. In the final stage, the released cells were then characterized for TCR expression level using Raman scattering.

3.2. Interrogation of synthetic pMHC-TCR interaction on-chip

To evaluate TCR-pMHC interaction on chip under ac-EHD flow condition, we first analyzed the interaction of commercially availed HRP labeled soluble TCR (p53 (aa264-272) Star™Multimer (HLA-A2.1 restricted)) and its cognate p53-MHC I molecule (biotinylated p53-HLA-A2). Prior to run ac-EHD experiments, we evaluated the effect of ac electric field on pMHC-TCR interaction by conducting electrochemical analysis and found minimal to no effect of the applied field on pMHC-TCR bindings (see supporting information for details, Figure S6) To perform on-chip experiment, we functionalized biotinylated pMHC molecules (monomer) on the chip surface using avidin-biotin chemistry. Different concentrations of HRP labelled soluble TCR solutions were then flown through the functionalized channel under applied ac electric field (f = 600 Hz and V_{pp} = 100 mV, calculated electric field = 2 mV/μm). In this case, we utilized an optimized ac-EHD condition used in our previous work [30] and used three different concentrations of TCR molecules (250 ng/mL, 500 ng/mL and 1 μg/mL) spiked in PBS (1 mM, pH 7.0). After completing the capture experiment, 3, 3′, 5, 5′-Tetramethylbenzidine (TMB) solution was driven through the channels to allow colorimetric reaction for 5 min and the resulting solution was collected from the outlet for absorbance measurements using a UV–vis spectrophotometer. Control experiments were done by flowing TCR solution through the non-pMHC functionalized device. As shown in Figure 2, the positive TCR-pMHC interaction with three different concentrations of TCR solution showed higher absorbance value in comparison to the control experiment. The lowest concentration for detection was found to be 250 ng/mL of HRP labeled TCR (average UV absorbance of 0.14 ± 0.02, $n = 3$). This data clearly demonstrates that our method is capable of interrogating TCR-pMHC interaction on chip with high specificity and sensitivity and may potentially be able to capture the antigen specific T-cells.

3.3. Specificity of the assay in capturing T-cells

To investigate the capture of antigen specific T-cells on pMHC functionalized immunochip under ac-EHD, we first generated $Hemagglutinin_{306\text{-}318}$ (HA) specific CD4+ T-cells form HLA-DRB1*04:01+ healthy control by following the standard protocol (see supplementary section for details). To confirm the presence of TCR expression on target HA-specific CD4+ cloned T-cells, we performed FACS analysis of PE-pMHC tetramer stained cells. The FACS data in Figure 3a clearly shows the TCR expression level in our HA-specific CD4+ cloned T-cells. We then

performed capture experiments with 500 CD4+ T-cells (prestained with DiO) in 1 mM PBS on anti-pMHC (monomer) functionalized device under optimized ac-EHD conditions (f = 600 Hz, Vpp = 100 mV) (see supplementary information for ac-EHD optimization, Figure S7) and counted the captured T-cell under a fluorescence microscope [34]. As a control to our ac-EHD flow system and to compare the capture performance, we also performed capture experiments using pressure driven flow system. Under these ac conditions, our system was able to isolate 33.58 ± 4.50% spiked T-cells whereas only 17.33 ± 2.02% capture efficiency was recorded when capture experiments were performed under pressure driven flow condition (i.e., no ac-EHD, Figure 3b). This data clearly demonstrated the feasibility of immunochip for T-cell capture using pMHC-TCR interaction.

To further improve the capture performance, we utilizedpMHC tetramer as capture agents instead of pMHC monomers due to their higher avidity toward TCRs on T-cells [9,35]. In this case, we used biotin streptavidin followed by anti-PE based functionalization procedure to ensure appropriate orientation of pMHC tetramers on the surface (Figure 4a, see supplementary information for more details, Figures S4, S8). To evaluate the on-chip capture efficiency, we then spiked 500 target CD4+T-cells in 1 mM PBS and the samples were driven through the tetramer functionalizeddevice. Under optimal ac-EHD condition (f = 600 Hz, V_{pp} = 100 mV), 56.93 ± 7.31% target cells were captured in a pMHC tetramer modified device in comparison to a monomer immobilized device (33.58 ± 4.50% of spiked T-cells) (Figure 4b). The increase in capture efficiency on a tetramer functionalized device might be the result of the stronger affinity of pMHC tetramer with multiple TCRs expressed on T-cell surfaces [9]. Control experiments by flowing target T-cells (spiked in 1 mM PBS) under ac-EHD through i) no-pMHC ii) anti-HER2 and iii) non-target pMHC functionalized immunochip showed minimal non-specific adsorption (<0.5%) which demonstrated the specificity of our system in capturing T-cell using pMHC-TCR interaction (Figure 4b).

3.4. Analytical performance of the device in capturing T-cells

To investigate the analytical performance of the system, PBS samples containing designated number of target CD4+ T-cells (i.e., 100, 200, 500, 750 and 1000) were subjected to capture experiments under optimized ac-EHD condition (V_{pp} = 100 mV and f = 600 Hz). Average number of cell captured were found to be 58.66 ± 2.60 (for 100 spiked cells), 108 ± 5.05 (for 200 spiked cells), 284.66 ± 7.31 (for 500 spiked cells), 424 ± 2.33 (for 750 spiked cells), and 562.33 ± 2.90 (for 1000 spiked cells), respectively. This data clearly indicates the dynamic range of the immunochip for capturing T-cells (i.e., 100–1000 T-cells) using pMHC-TCR interaction (Figure 5a). However, experiments with T-cell number below 100 spiked cells in 1 mM PBS did not show reproducible capture efficiency. Thus we conclude that the limit of detection for our microfluidic platform is 100 cells. To test the efficacy of our method in capturing T-cells from complex mixtures, we spiked different number of T-cells (100, 500 and 1000) in 10^6 healthy PBMCs and flown through our system. As shown in Figure 5b, our system provided high sensitivity (0.005%) for T-cell isolation from complex biological fluid (Figure 5b). This level of sensitivity is comparable with the existing standard techniques for T-Cell isolation (Table 1) [11,12,36].

3.5. TCR expression analysis of T-cells

In order to analyze TCR expression level, captured T-cells were labelled with pMHC-SERSnanotag on chip (see supplementary information for pMHC-SERSnanotag preparation). SERS labelled T-cells were then released from the microfluidic device by applying 1.4 V DC electric pulse for 200 s.

In our previous work, we already showed that this optimised DC pulse successfully released cells from the device [26]. Released cells were then subjected to SERS measurement to record the signal from responsive cells. Approximately 200 spectra were recorded for each sample and analyzed to extract average TCR expression level (SERS signal intensity is proportional to TCR expression level due to the pre-labelling of cells with SERS nanotag). As shown in Figure 6a,b, average TCR expression of bulk T-cells in solutions (1 mM PBS) increased proportionally with increasing number of T-cells. In contrast, the control experiments with nonspecific pMHC-SERS nanotag showed negligible signal for TCR expression. Furthermore, the frequency vs intensity curve for 1000 T-cells shown in Figure 6c provided a clear heterogeneous distribution of TCR expression in comparison to the control experiment without target pMHC. This data suggest that our method may potentially be able to monitor the heterogeneity in T-cell TCR population which could significantly facilitate the clinical outcome.

To further analyze the diversity in TCR expression level in single T-cell, we characterized TCR expression level of individual T-cell following a protocol explored by Choo and co-workers for cell surface protein analysis [37]. In our experiment, released T-cells were placed on a plain glass surface and scanned individually by the Raman microscope. Figure 6d shows false color SERS mapping images of three representative T-cells and their average SERS intensities representing the TCR expression levels of the corresponding cells. These data further clarify that TCR expression levels are highly heterogeneous in antigen specific T-cells. Since activation and function of T-cells depends on the level of TCR expression and its interaction with specific pMHC presented by antigen presenting cells, this information could be highly important for clinical application [38]. This information could be of further use to design new therapeutic formulations and improve existing ones. However, further experiments with different T-cell populations need to be performed to precisely validate the diversity among individual T-cells within the same population.

4. CONCLUSION

We reported a simple technique for detection and characterization of antigenspecific T-cells by combing ac-EHD enabled microfluidic platform with a sensitive SERS based detection system. To the best of our knowledge, this is the first demonstration of a miniaturized microfluidic system for antigen specific immune cell isolation and subsequent characterization of their TCR expression using SERS barcoding. As a proof-of-concept study, our system was able to isolate $56.93 \pm 7.31\%$ of target antigen specific T-cells from a complex mixture with high specificity and sensitivity (0.005%). Furthermore, the use of SERS nanotag labelling enabled the screening of TCR expression on bulk T-cell samples as well as on individual T-cell surface which can potentially inform on the T-cell activity under certain diseased conditions. We envisage that the developed method will be of interest for antigen specific T-cell detection and characterization as well as for monitoring the adaptive immune therapy in clinics.

CONFLICTS OF INTEREST

There are no conflicts to declare.

Table 1.

pMHC arrays for T-cell analysis.

Platform	Detection limit	Reference
Microarray with pMHC tetramer coated slide and fluorescence detection.	Detection limit 0.1% for CD8 T-cells, can screen 7 different antigen specific T-cells per assay.	Soen et al. (2003)
Microarray co-spotted with dimeric pMHCs and anti-cytokine antibodies. Fluorescence based detection.	Detection limit 0.01% for CD8 T-cells, 7 different CD8 T-cell population can be assayed.	Chen et al. (2005)
Microarray of co-spotted pMHCs, anti-cytokine antibodies and costimulatory molecules. Fluorescence based detection.	Detection limit 0.1% for CD8 T-cells.	Stone et al. (2005)
pMHC microarray immobilized on antibody spotted polyacrylamide microscopy slide and fluorescence based detection.	Detection limit 0.01% for CD8 T-cells.	Deviren et al. (2007)
Microarray containing DNA probed pMHCs immobilized on complementary DNA probe printed glass slide and fluorescence based detection.	Detection limit 0.1% for CD8 T-cells, 3 different antigen specific T-cells can be screened per assay.	Kwong et al. (2009)
pMHC tetramer microarray and fluorescence based detection.	Detection limit 0.02% for CD8 T-cells, >40 specific T-cells can be screened.	Brooks et al. (2015)
Staining of T-cells with DNA barcode labelled pMHC and detection by sequencing	Detection limit 0.002% for CD8 T-cells, 1031 different antigen specific T-cells can be screened per assay	Bentzen et al. (2016)
Mass cytometry	Detection limit 0.001% for $CD8^+$ T cells with ability to assay 109 different T-cells per assay.	Newell et al. (2013)
Flow cytometry	Not reported	Klinger et al. (2015)
AAPC-microplate for T-cells isolation using pMHC and anti- CD28 coated magnetic beads followed by optical microscopy and ELISPOT for cell counting and secretion analysis.	Detection limit 0.001% for $CD8^+$T-cells.	Shen et al. (2017)
pMHC array for T-cell isolation and hemin functionalized reduced graphene oxide (HRGO)/pMHCmultimers for colorimetric detection.	Not reported	Zhu et al. (2018)
pMHC dodecamer based T-cell staining and flow cytometry based analysis.	Not reported, can detect low affinity TCR-pMHC interaction often not possible for tetramer based techniques	Huang et al. (2016)

Figure 1.

Schematic representation of isolation and analysis of T-cells using pMHC-TCR interaction enabled by electric field induced T-cell capture, cell release under DC pulse and TCR expression analysis using designated SERS-nanotags.

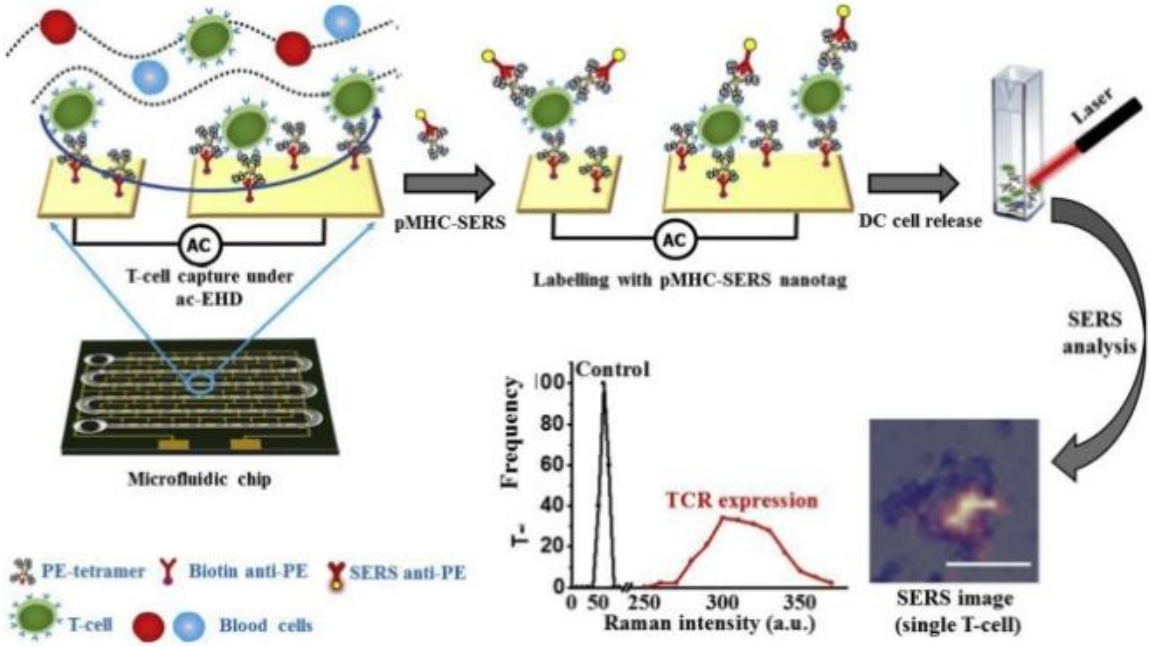

Figure 2.

On chip interrogation of pMHC-TCR interaction under ac-EHD field (V_{pp} = 100 mV, f = 600 Hz). (a) Colorimetric detection of captured soluble TCR tetramer (250 ng/ mL – 1 µg / mL) in PBS under ac-EHD field. (b) Corresponding UV–vis absorption spectra obtained from respective colorimetric solutions.

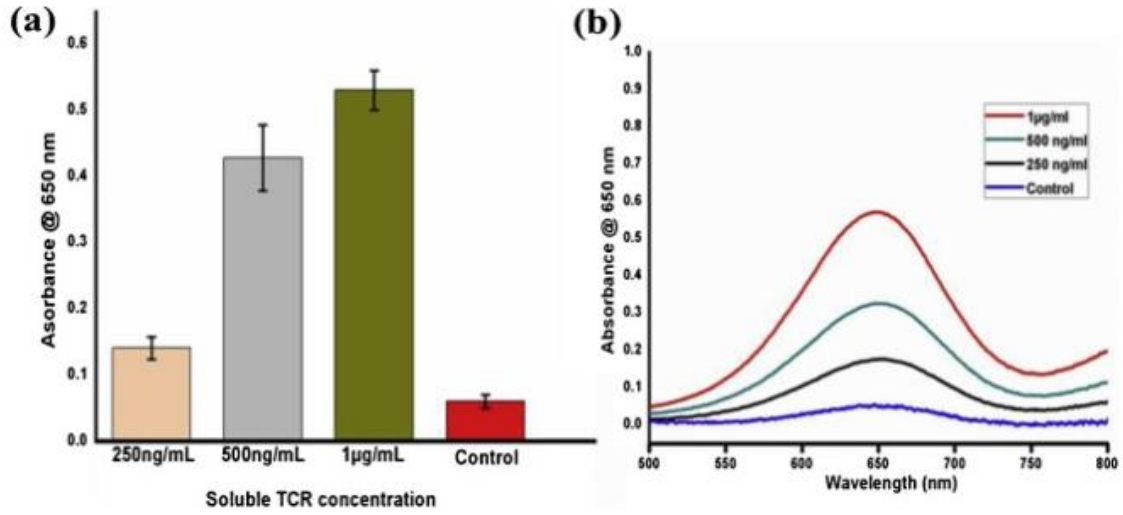

Figure 3.

(a) Flow cytometry analysis of HA + CD4+T-cell clones with (left) no tetramerstaining (control) and (right) PE labeled pMHCII tetramer staining; (b) Capture efficiency of CD4+ T-cells (500 T-cells spiked in 1 mM PBS) on monomer functionalized immunochip under ac-EHD and pressure (no ac-EHD) flow conditions. (c) Representative fluorescence images of captured T-cells under ac-EHD (top) and pressure driven flow conditions (bottom). Scale bar is 20 μm.

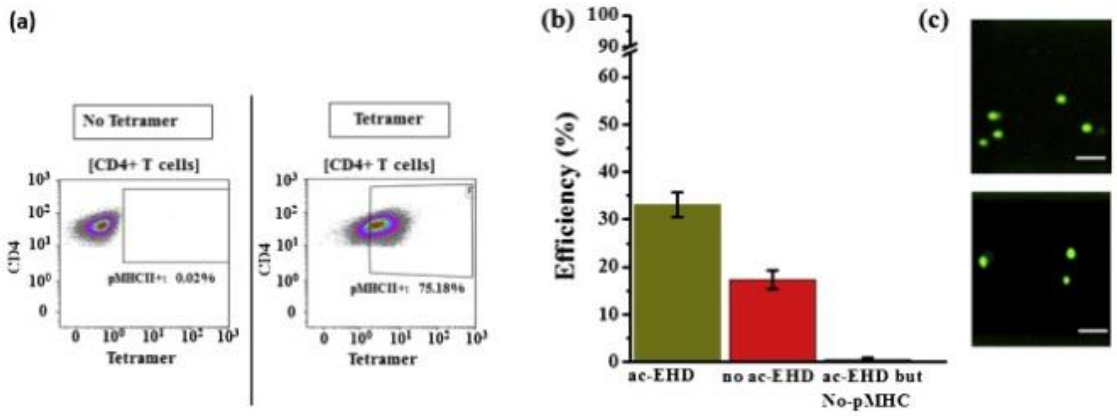

Figure 4.

(a) Schematic illustration of T-cell capture on pMHCtetramer functionalized device; (b) Capture performance of ac-EHD device functionalized with target specific pMHC monomer (olive bar) and tetramer (red bar) for T-cell isolation. Control experiments with no-pMHC, nonspecific antibody(anti-HER2) and non-target pMHC tetramer showed negligible signal (For interpretation of the references to colour in this figure legend, the reader is referred to the web version of this article

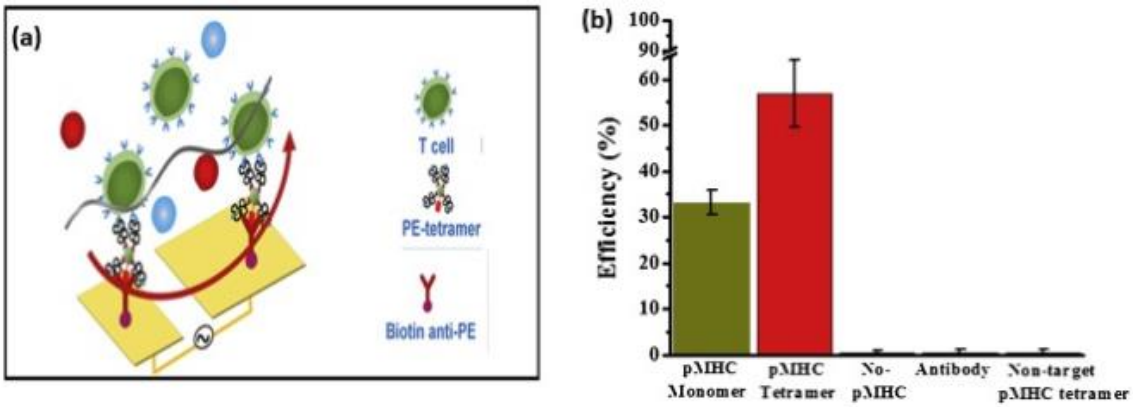

Figure 5.

Sensitivity of the immunochip (a) Dynamic range of the assay for capturing T-cell spiked in 1 mM PBS under ac-EHD condition, n = 3. (b) Capture performance of ac-EHD microfluidic assay in capturing designated number (100, olive bar; 500, green bar; 1000, red bar) of T-cells in presence of a large number (10^6 cells) non-target peripheral blood mononuclear cells, n = 3 (For interpretation of the references to colour in this figure legend, the reader is referred to the web version of this article)

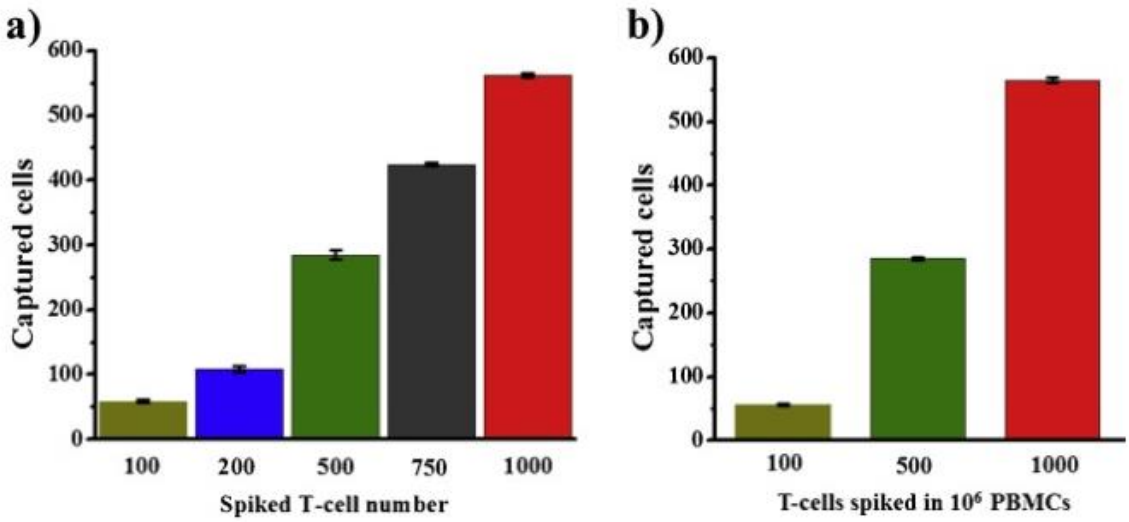

Figure. 6.

(a) SERS spectra for TCR expression on designated number of T-cells ranging from 1000 to 5000 cells/mL and (b) Average SERS signal for 1000–5000 T-cells numbers, (n = 3), signal to noise ratio of SERS signals for all three T-cell concentrations measured are 9.01, 20.83 and 27.90, respectively. (c) Frequency distribution of TCR expression among T-cells (for 1000 T-cells) and (d) SERS mapping images of individual T-cells (top) and their corresponding SERS spectra (bottom) showing the level of TCR expression (represented by SERS intensity) on individual T-cells. Scale bar is 10 μm.

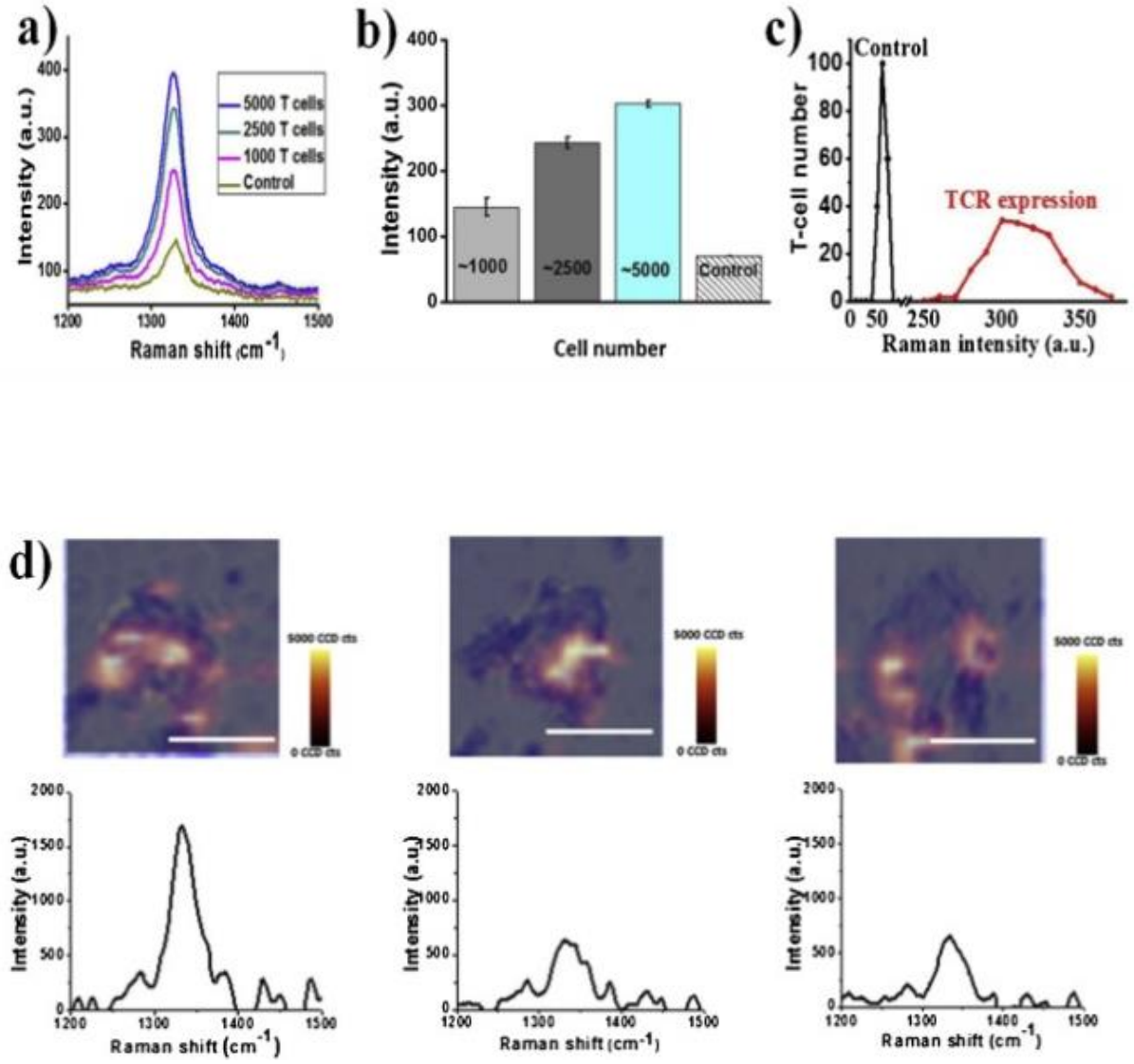

REFERENCES

1. N. Labrecque, L.S. Whitfield, R. Obst, C. Waltzinger, C. Benoist, D. Mathis. **How much TCR does a T cell need?** Immunity, 15 (2001), pp. 71-82

2. R.H. Schwartz. **Historical overview of immunological tolerance.** Cold Spring Harb. Perspect. Biol., 4 (2012), Article a006908

3. A.N. Houghton, J.A. Guevara-Patiño. **Immune recognition of self in immunity against cancer.** J. Clin. Invest., 114 (2004), pp. 468-471

4. D.R. Fooksman, S. Vardhana, G. Vasiliver-Shamis, J. Liese, D.A. Blair, J. Waite, *et al*. **Functional anatomy of T cell activation and synapse formation**. Annu. Rev. Immunol., 28 (2010), pp. 79-105

5. M. Lever, P.K. Maini, P.A. Van Der Merwe, O. Dushek. **Phenotypic models of T cell activation**. Nat. Rev. Immunol., 14 (2014), pp. 619-629

6. R.H. McMahan, J.A. McWilliams, K.R. Jordan, S.W. Dow, D.B. Wilson, J.E. Slansky. **Relating TCR-peptide-MHC affinity to immunogenicity for the design of tumor vaccines**. J. Clin. Invest., 116 (2006), pp. 2543-2551

7. S. Zhong, K. Malecek, L.A. Johnson, Z. Yu, E.V.-S. de Miera, F. Darvishian, *et al*. **T-cell receptor affinity and avidity defines antitumor response and autoimmunity in T-cell immunotherapy**. Proc. Natl. Acad. Sci., 110 (2013), pp. 6973-6978

8. D.K. Cole, K.M. Miles, F. Madura, C.J. Holland, A.J. Schauenburg, A.J. Godkin, *et al*. **T-cell receptor (TCR)-peptide specificity overrides affinity-enhancing TCR-major histocompatibility complex interactions**. J. Biol. Chem., 289 (2014), pp. 628-638

9. J.D. Altman, P.A. Moss, P.J. Goulder, D.H. Barouch, M.G. McHeyzer-Williams, J.I. Bell, *et al*. **Phenotypic analysis of antigen-specific T lymphocytes**. Science, 274 (1996), pp. 94-96

10. T.F. Greten, J.E. Slansky, R. Kubota, S.S. Soldan, E.M. Jaffee, T.P. Leist, *et al.* **Direct visualization of antigen-specific T cells: HTLV-1 Tax11–19-specific CD8+ T cells are activated in peripheral blood and accumulate in cerebrospinal fluid from HAM/TSP patients**. PNAS, 95 (1998), pp. 7568-7573

11. E.W. Newell, N. Sigal, N. Nair, B.A. Kidd, H.B. Greenberg, M.M. Davis. **Combinatorial tetramer staining and mass cytometry analysis facilitate T-cell epitope mapping and characterization**. Nat. Biotechnol., 31 (2013), p. 623

12. A.K. Bentzen, A.M. Marquard, R. Lyngaa, S.K. Saini, S. Ramskov, M. Donia, *et al.* **Large-scale detection of antigen-specific T cells using peptide-MHC-I multimers labeled with DNA barcodes**. Nat. Biotechnol., 34 (2016), p. 1037

13. J. Huang, X. Zeng, N. Sigal, P.J. Lund, L.F. Su, H. Huang, *et al*. **Detection, phenotyping, and quantification of antigen-specific T cells using a peptide-MHC dodecamer**. PNAS, 113 (2016) E1890-E7

14. G.A. Kwong, C.G. Radu, K. Hwang, C.J. Shu, C. Ma, R.C. Koya, *et al.* **Modular nucleic acid assembled p/MHC microarrays for multiplexed sorting of antigen-specific T cells**. J. Am. Chem. Soc., 131 (2009), pp. 9695-9703

15. C. Phetsouphanh, J.J. Zaunders, A.D. Kelleher. **Detecting antigen-specific T cell responses: from bulk populations to single cells**. Int. J. Mol. Sci., 16 (2015), pp. 18878-18893

16. Y. Soen, D.S. Chen, D.L. Kraft, M.M. Davis, P.O. Brown. **Detection and characterization of cellular immune responses using peptide–MHC microarrays**. PLoS Biol., 1 (2003), p. e65

17. D.S. Chen, Y. Soen, T.B. Stuge, P.P. Lee, J.S. Weber, P.O. Brown, *et al*. **Marked differences in human melanoma antigen-specific T cell responsiveness after vaccination using a functional microarray**. PLoS Med., 2 (2005), p. e265

18. G. Deviren, K. Gupta, M.E. Paulaitis, J.P. Schneck. **Detection of antigen-specific T cells on p/MHC microarrays**. J. Mol. Recognit., 20 (2007), pp. 32-38

19. C. Yue, M. Oelke, M. Paulaitis, J. Schneck. **Novel cellular microarray assay for profiling T-cell peptide antigen specificities**. J. Proteome Res., 9 (2010), pp. 5629-5637

20. S.E. Brooks, S.A. Bonney, C. Lee, A. Publicover, G. Khan, E.L. Smits, *et al*. **Application of the pMHC array to characterise tumour antigen specific T cell populations in leukaemia patients at disease diagnosis**. PLoS One, 10 (2015), Article e0140483

21. C. Shen, T. Xu, Y. Wu, X. Li, L. Xia, W. Wang, *et al*. **Frequency and reactivity of antigen-specific T cells were concurrently measured through the combination of artificial antigen-presenting cell, MACS and ELISPOT**. Sci. Rep., 7 (2017), p. 16400

22. J. Zhu, Y. Li, L. Li, J. Wang, H. Wang, W. Hong, *et al*. **A novel absorption spectrometric method, based on graphene nanomaterials, for detection of hepatocellular carcinoma-specific T lymphocyte cells**. Int. J. Nanomed., 13 (2018), p. 5523

23. A.K. Bentzen, S.R. Hadrup. **Evolution of MHC-based technologies used for detection of antigen-responsive T cells, cancer immunology**. Immunotherapy, 66 (2017), pp. 657-666

24. J.M. Jackson, M.A. Witek, J.W. Kamande, S.A. Soper. **Materials and microfluidics: enabling the efficient isolation and analysis of circulating tumour cells**. Chem. Soc. Rev., 46 (2017), pp. 4245-4280

25. K. Ward, Z.H. Fan. **Mixing in microfluidic devices and enhancement methods**. J. Micromech. Microeng., 25 (2015), Article 094001

26. S. Dey, R. Vaidyanathan, L.G. Carrascosa, M.J. Shiddiky, M. Trau. **Electric field induced isolation, release, and recapture of tumor cells**. ACS Sens., 1 (2016), pp. 399-405

27. M.J. Shiddiky, R. Vaidyanathan, S. Rauf, Z. Tay, M. Trau. **Molecular nanoshearing: an innovative approach to shear off molecules with AC-induced nanoscopic fluid flow**. Sci. Rep., 4 (2014), p. 3716

28. K. Kamil Reza, J. Wang, R. Vaidyanathan, S. Dey, Y. Wang, M. Trau. **Electrohydrodynamic-induced SERS immunoassay for extensive multiplexed biomarker sensing**. Small, 13 (2017), Article 1602902

29. X.-M. Qian, S. Nie. **Single-molecule and single-nanoparticle SERS: from fundamental mechanisms to biomedical applications**. Chem. Soc. Rev., 37 (2008), pp. 912-920

30. S.C.-H. Tsao, J. Wang, Y. Wang, A. Behren, J. Cebon, M. Trau. **Characterising the phenotypic evolution of circulating tumour cells during treatment.** Nat. Commun., 9 (2018), p. 1482

31. Brown, C. Smith, A. Rennie. **Pumping of water with ac electric fields applied to asymmetric pairs of microelectrodes**. Phys. Rev. E, 63 (2000), Article 016305

32. R.J. Hunter. **Foundations of Colloidal Science**. Oxford University Press Inc (1987)

33. S.W. Scally, J. Petersen, S.C. Law, N.L. Dudek, H.J. Nel, K.L. Loh, *et al*. **A molecular basis for the association of the HLA-DRB1 locus, citrullination, and rheumatoid arthritis**. J. Exp. Med., 210 (2013), pp. 2569-2582

34. S.C.-H. Tsao, R. Vaidyanathan, S. Dey, L.G. Carrascosa, C. Christophi, J. Cebon, *et al*. **Capture and on-chip analysis of melanoma cells using tunable surface shear forces**. Sci. Rep., 6 (2016), p. 19709

35. L. Wooldridge, A. Lissina, D.K. Cole, H.A. Van Den Berg, D.A. Price, A.K. Sewell. **Tricks with tetramers: how to get the most from multimeric peptide–MHC**. Immunology, 126 (2009), pp. 147-164

36. M. Klinger, F. Pepin, J. Wilkins, T. Asbury, T. Wittkop, J. Zheng, *et al*. .**Multiplex identification of antigen-specific T cell receptors using a combination of immune assays and immune receptor sequencing**. PLoS One, 10 (2015), Article e0141561

37. S. Lee, H. Chon, J. Lee, J. Ko, B.H. Chung, D.W. Lim, *et al*. **Rapid and sensitive phenotypic marker detection on breast cancer cells using surface-enhanced Raman scattering (SERS) imaging**. Biosens. Bioelectron., 51 (2014), pp. 238-243

38. G.P. Morris, P.M. Allen. **How the TCR balances sensitivity and specificity for the recognition of self and pathogens**. Nat. Immunol., 13 (2012), pp. 121-128